

Mary Ann Jenkins¹ * Ruiyu Sun² Steven K. Krueger² Joseph J. Charney³ and Michael A. Zulauf²

¹York University, Toronto, Canada

²University of Utah, Salt Lake City, Utah

³United States Forest Service, North Central Research Station, East Lansing, MI

1. Introduction

It is observed that the presence of vertical shear, especially at low levels, in the ambient atmosphere is important to wildfire behavior. Byram (1954), based on available observational data, suggested that low-level jets, usually not more than 300 m AGL, or ambient wind profiles with wind speed decreasing with height (with the possible exception of the first hundred metres), along with ambient wind speeds of 8 m/s or more at the elevation of the fire, favor extremely erratic wildfire behavior.

The intense vorticity observed in wildfires plays an important role in the evolution of such extreme wildfire behavior as the development of fire whirls in and ahead of the fire front, erratic and/or accelerated fire spread, and massive or area ignition by firebrand spotting. Current knowledge provides limited guidance to wildfire managers and fire fighters on how severe fire convection will evolve in a given environment. Background wind profiles with near-surface shear have been used in several numerical studies (e.g., Clark et al., 1996, Trelles et al., 1999, Cunningham et al., 2005, etc.) to explore the generation and evolution of vortical features of buoyant plumes in this type of wind environment. These numerical studies are an attempt to determine the dependence of vortical features on observable environmental parameters such as intensity of heat source, shear of ambient atmospheric winds, and basic-state stratification.

There is still uncertainty exactly what processes involving shear in the background flow are responsible, either directly or indirectly, for the generation and development of vortical features in wildfire. Cunningham et al. (2003), for example, suggest that horizontal vorticity associated with near-surface vertical shear in the ambient wind may be converted into vertical vorticity near the ground via tilting by convection in the vicinity of the fire. Studies like these are focused mainly on the development of coherent vortical features in plumes of stationary fires. Clark et al. (1996) disregard tilting of near-surface ambient wind shear as a mechanism for

vorticity generation important erratic and/or dangerous to fire behavior, and emphasize instead the transport of fire vorticity by the background wind profile and the impact of this vorticity on fire-line behavior and spread when it re-enters the fire. Trelles et al. (1999) show that vertical shear in the background wind affects plume rise heights and vortical structure.

This study is one of the first systematic investigations of the effects of ambient vertical wind shear on the behavior of non-stationary wildland fires. The goal is to explore what processes involving shear in the background flow are likely important to, or responsible for, erratic and dangerous fire behavior in the fire domain.

The UU-LES (University of Utah's Large Eddy Simulator) wildfire coupled model (Sun et al., 2007) is used to examine the effect of several background wind profiles on the development of horizontal north-south vorticity in a grassfire. The simulations are of moving surface grass fires, burning in uniform fuel on level terrain, initialized as straight fire lines perpendicular to the direction of background the wind. Several grassfire simulations for different background wind profiles chosen to match Byram's most dangerous wind profile category were completed. The following is a report on the results of three exploratory simulations.

2. Linear Theory

The simplest way to represent the impact of shear in the background flow is to use linear theory to model the effects of the environmental wind on a convective fire updraft and examine the x , y , and z vorticity components in a 3-D velocity field. Here $\vec{u} = \vec{v} + \hat{k}w$ is the 3-d velocity field, $\vec{\omega} = \nabla \times \vec{u}$ is the 3-D vorticity field, no Coriolis force is considered, and $\nabla = \frac{\partial}{\partial x_i}$, $i = 1, 2, 3$. The Boussinesq approximation is made, where $\nabla \cdot \vec{u} = 0$ and $b \equiv -g \frac{\rho'}{\rho_0}$ is the total buoyancy for constant base state density ρ_0 .

Imagine a flow field consisting of a convective updraft embedded in \overline{U} , a basic state east-west flow that is a function of height z only. Let

$$\vec{\omega} = \frac{d\overline{U}}{dz} \hat{j} + \vec{\omega}'(x, y, z, t), \quad \vec{u} = \overline{U} \hat{i} + \vec{u}'(x, y, z, t). \quad (1)$$

*Corresponding author address: Department of Earth and Space Science and Engineering, York University, Toronto, ON, Canada, M3J 1P3. E-mail: maj@yorku.ca

Note that $S = \frac{d\bar{U}}{dz}\hat{j}$ is horizontal y vorticity in the background flow. Primed quantities ($'$) represent perturbations due to fire convection.

In this study the effect of \bar{U} and S on the development of the horizontal y -vorticity ζ_y is examined. The horizontal y -vorticity equation can be written

$$\frac{\partial \zeta_y}{\partial t} = \hat{j} \cdot \left[\nabla \times (\bar{u} \times \bar{\omega}) + \nabla \times (b\hat{k}) \right], \quad (2)$$

where $\zeta_y = \hat{j} \cdot \bar{\omega} = \hat{j} \cdot \nabla \times \bar{u}$. The \hat{j} component of the first term on the right-hand side (RHS) of the *linearized* horizontal y vorticity Equation (2) is

$$\hat{j} \cdot \nabla \times \left(-w' S \hat{i} + \left[\bar{U} \zeta_y' + \bar{U} S + u' S \right] \hat{k} \right). \quad (3)$$

The linearized vorticity tendency for the y component of vorticity is therefore

$$\frac{\partial \zeta_y'}{\partial t} = -\bar{U} \frac{\partial \zeta_y'}{\partial x} - S \left[\frac{\partial u'}{\partial x} + \frac{\partial w'}{\partial z} \right] - w' \frac{dS}{dz} - \frac{\partial b}{\partial x}. \quad (4)$$

The first term on the RHS of Equation (4) is advection of perturbed vorticity ζ_y' by the basic flow, the second term is the generation of ζ_y' by divergence in the perturbed x - z flow, the third term represents the effect of an inflection point in the basic state wind profile coupled with vertical motion due to the fire, and the final term is the generation of ζ_y' by b .

If \bar{U} has a vertical structure such as Clark et al. (1996)'s hyperbolic tangent profile of \bar{U} (that varied from 3 m/s near the ground, changed sign at $z=500$ m, and was asymptotic to -3 m/s aloft), then fire-generated vorticity can be advected back into the fire, increasing the probability of erratic fire behavior. Byram (1954) also classified this type of ambient wind profile (i.e., winds decreasing with height near the ground) as well correlated with extreme fire behavior. If S exists and is significant, then convergence/divergence by $\frac{\partial u'}{\partial x} + \frac{\partial w'}{\partial z}$ in the fire's convection column can generate ζ_y' . If S has an inflection or 'jet' point — described by Byram (1954) as a common feature of ambient wind profiles associated with extreme fire behavior — then large w' is capable of generating ζ_y' near the inflection point. If S or \bar{U} does not exist, then the only linear term that initiates ζ_y' is buoyancy.

Likewise the linearized vorticity tendency for the x component of vorticity is

$$\frac{\partial \zeta_x'}{\partial t} = -\bar{U} \frac{\partial \zeta_x'}{\partial x} + S \frac{\partial v'}{\partial x} + \frac{\partial b}{\partial y}. \quad (5)$$

The first term on the RHS of Equation (5) is advection of perturbed vorticity ζ_x' by the basic flow, the second term is the generation of ζ_x' by tilting of vertical vorticity due to $\frac{\partial v'}{\partial x}$ into the x direction by the background

shear S . If S or \bar{U} does not exist, then the only linear term that initiates ζ_x' is buoyancy.

Likewise the linearized vorticity tendency for the z component of vorticity is

$$\frac{\partial \zeta_z'}{\partial t} = -\bar{U} \frac{\partial \zeta_z'}{\partial x} + S \frac{\partial w'}{\partial y}. \quad (6)$$

The first term on the RHS of Equation (5) is advection of perturbed vorticity ζ_z' by the basic flow, the second term is the generation of ζ_z' by tilting of vertical vorticity due to $\frac{\partial w'}{\partial y}$ into the z direction by the background shear S . If S or \bar{U} does not exist, then no linear term initiates ζ_z' .

In a mature fire the perturbed wind is usually much stronger than the mean wind, and nonlinear terms are not negligible. Linear theory applies therefore to the very initial stages of fire convection and explains only limited growth. The reason for severe and erratic fire behavior must lie in the nonlinear terms (and therefore a full 3-D Navier Stokes Large Eddy Simulation approach is necessary), as the perturbations modify the mean flow and the vorticity gradients. Nonetheless, Equations (4), (5), and (6) isolate the effects of environmental parameters \bar{U} and S on the development of fire vorticity components ζ_y' , ζ_x' , and ζ_z' , respectively.

3. Numerical Experimental Set-up

Readers are referred to Sun et al. (2007) and Zulauf (2001) for details on the UU-LES wildfire coupled model used in this study. In each of the three simulations the domain size was $(x, y, z) = (3200 \text{ m}, 1600 \text{ m}, 11000 \text{ m})$, covered by a grid mesh of $(x, y, z) = (640, 320, 81)$ nodes. A vertically-stretched grid was used, with a minimum vertical (z) grid size of 5 m at the surface. Moving surface grass fires, burning in uniform fuel on level terrain, initialized as a straight line perpendicular to the direction of the wind, and located 1500 m in the x direction from the origin, determined the source of buoyancy. Each coupled UU-LES simulation lasted 15 minutes. A uniform base-state potential temperature of 300°C was used. Initial fireline length and width were 400 and 10 m, respectively. Fuel load was 0.626 kg/m². The atmosphere was dry. The initial roughness height was 0.036 m. A roughness height of 0.006 was used after the fuel was burnt. Each simulation was identical except for the background wind field. The mean wind profiles used in the study are shown in Figure 1. Experiment 'GLM-C' is the 'control' run, in which a constant background wind of 5.5 m/s was used, experiment 'GLM-LS' is the 'linear-shear' run, in which a linearly sheared background wind was used, and experiment 'GLM-TH' is the 'tanh' run, in which

a tanh-sheared background wind was used. In all simulations the environmental surface wind speed was 5.5 m/s.

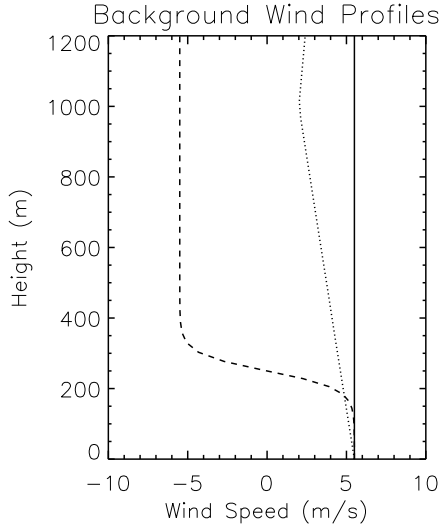


Figure 1: Vertical profiles of background winds used in coupled UU-LES Experiments GLM-C (solid line), GLM-LS (dotted line), GLM-TH (dashed line).

4. Simulation Results

Figures 2, 3, and 4 show the coupled UU-LES results of fire simulation GLM-C. This is the ‘control’ simulation. Figure 2 shows an almost symmetrical fire plume in terms of the ζ_x , vertical velocity w , and linear vorticity terms in Equation (5). Although generation of ζ'_x by the buoyancy term is significant in the first ~ 200 m AGL, the advection of ζ'_x by the background wind is seen to have a larger impact on the generation of ζ'_x . Figure 3 shows relatively strong ζ_y and vertical velocity w fields well contained within a relatively narrow fire plume that tilts slightly downwind (eastward or positive x direction) of the moving fire line. Although generation of ζ'_y by the buoyancy term in Equation (4) is significant in the fire plume, the effect of the advection term in Equation (4), is seen to have a considerably larger impact on the generation of ζ'_y . Figure 4 shows coherent vertical vortices at the leading edge of the fire plume with a well developed convective updraft between them. The generation of ζ'_z by the advection term in Equation (6) is noticeable, but not particularly significant or widespread.

Figures 5, 6, and 7 show the coupled UU-LES results of fire simulation GLM-LS. This is the ‘linear-shear’ simulation. Figure 5 shows a coherent and an almost

symmetrical fire plume in terms of the ζ_x , vertical velocity w , and linear vorticity terms in Equation (5). As in Figure 2, although the generation of ζ'_x by the buoyancy term is significant in the first ~ 200 m AGL, the effect of the advection of ζ'_x by the background wind is seen to have a larger impact on the generation of ζ'_x . Compared to Figure 2, both advection and buoyancy terms are slightly more significant in this case. Figure 6 shows again relatively strong ζ_y and vertical velocity w fields well contained within the fire plume, which is now more widespread, less narrow and concentrated, and tilting straight up. Except for no eastward tilt, the buoyancy and advection terms in this simulation look similar in magnitude and extent to those in GLM-C. Figure 7 shows again coherent vertical vortices at the leading edge of the fire plume with a well developed convective updraft between them. The generation of ζ'_z by advection is noticeable, but not particularly significant. Compared to GLM-C, advection and buoyancy terms are slightly more significant in this case. The most significant difference between simulations GLM-C and GLM-LS is that the fire line did not spread as far in the positive x direction (eastward) in GLM-LS as it did in GLM-C.

Figures 8, 9, and 10 show the coupled UU-LES results of fire simulation GLM-TH. This is the ‘tanh’ simulation. Compared to the results in Figures 2 and 5, the fire plume is completely noncoherent, with widespread and erratic behavior for ζ_x , vertical velocity w , and the linear vorticity terms in Equation (5). The buoyancy and advection terms in this simulation are entirely different in magnitude and extent to those in GLM-C and GLM-LS. The generation of ζ'_x and ζ'_y by the buoyancy terms in Equations (4) and (5) are not significant. The effect of the advection of $\zeta'_{x,y,z}$ by the mean wind is seen to have an enormous impact on the generation of $\zeta'_{x,y,z}$. The generation of ζ'_x and ζ'_y by the buoyancy terms in Equations (4) and (5) are just not important. Compared to the results in Figures 3 and 6, the results in Figure 9 show completely different evolutions of the ζ_y and vertical velocity w fields, not just in the fire plume, but throughout the entire model domain. In this case, the ζ_y and w are not concentrated only along the fire line, but are widespread and substantial in magnitude. Figure 10 no longer shows coherent vertical vortices at the leading edge of the fire plume with a well developed convective updraft between them. According to the w field — with extremely strong, widespread updrafts and downdrafts — the fire line has been pushed well back in the negative x direction (westward) in this simulation. This simulation represents severe and erratic fire behavior.

Note that in the Figures discussed here, the generation of $\zeta_{x,y,z}$ by tilting of vorticity terms in Equations

(5) and (6) or by divergence terms in Equations (4) and (5) is not reported. The impact of these terms on vorticity generation is the same order of magnitude as the impact of buoyancy.

5. Conclusions

The goal of this study is to provide guidance to wildfire managers and fire fighters on how severe fire convection will evolve in a given environmental wind shear. This study has numerically simulated three grass line fires, burning in flat terrain, in a neutral atmosphere, each with a simple but different uni-directional background vertical wind profile. The results of the study suggests that the behavior of the fire plume — development of updrafts and downdrafts and evolution of vorticity in the fire domain — and fire spread can be influenced greatly by vertical shear in the ambient wind. A constant background wind does not promote erratic or extreme fire behavior. The fire plume is well behaved, vorticity and vertical velocities are more-or-less steady-state, coherent in structure, and fire spread is steady in the direction of the surface wind. Similarly, a moderate background wind decreasing steadily with height with a small amount of vertical shear does not promote erratic or extreme fire behavior. It does, however, decrease, at least slightly, forward fire spread. The fire plume is well behaved, vorticity and vertical velocities are more-or-less steady-state, coherent in structure, and fire spread is steady in the direction of the surface wind. A background tanh-shaped wind with large low-level wind shear, decreasing with height, appears to be a 'dangerous' wind profile. Even though the surface wind is moderate in magnitude (e.g., ~ 5 m/s), the results of this study suggest that this type of background wind profile is capable of generating extremely erratic grassfire behavior and fire spread. It is advection of vorticity by the background flow, not tilting of horizontal vorticity associated with ambient wind shear, that influences this fire behavior.

A comprehensive reporting on these and other grassfire simulations (e.g., longer fire line length, different initial fire line geometries, etc.) in different background wind profiles (e.g., with an inflection point or low-level jet, etc.) is planned. These cases will explore in more detail the development of fire plume dynamics, vorticity and vertical motion, and fire spread and fire line evolution.

ACKNOWLEDGMENTS. This research was supported by the United States Department of Agriculture Forest Service Research Joint Venture Agreement 03-JV-11231300-08. A gratis grant of computer time from the Center for High Performance Computing, Univer-

sity of Utah, is gratefully acknowledged.

References

- Byram, G., 1954: Atmospheric conditions related to blowup fires. Technical Report Station Paper No. 35, USDA Forest Service, Southeastern Forest Experiment Station.
- Clark, T., M. Jenkins, J. Coen, and D. Packham, 1996: A coupled atmosphere-fire model: Role of the convective froude number and dynamic fingering at the fireline. *International J. Wildland Fire*, **6**, 177–190.
- Cunningham, P., S. Goodrick, M. Hussaini, and R. Linn, 2005: Coherent vortical structures in numerical simulation of buoyant plumes from wildfires. *International J. Wildland Fire*, **14**, 61–75.
- Cunningham, P., S. Goodrick, M. Hussaini, R. Linn, and C. Xia, 2003: Dynamics of fire plumes in vertical shear. *CD-ROM Preprints, Fifth Symp. on Fire and Forest Meteorology, Orlando, FL*.
- Sun, R., S. Krueger, M. Jenkins, and J. Charney, 2007: The importance of fire/atmosphere coupling and boundary layer turbulence to wildfire spread. *International J. Wildland Fire*, **submitted**.
- Trelles, J., K. McGrattan, and H. Baum, 1999: Smoke transport by sheared winds. *Combust. Theory Modelling*, **3**, 323–341.
- Zulauf, M., 2001: *Modeling the effects of boundary layer circulations generated by cumulus convection and leads on large-scale surface fluxes*. PhD thesis, University of Utah.

X Vorticity Budget Time[h:m:s]= 0:15: 0 Section at x(km)= 3.2

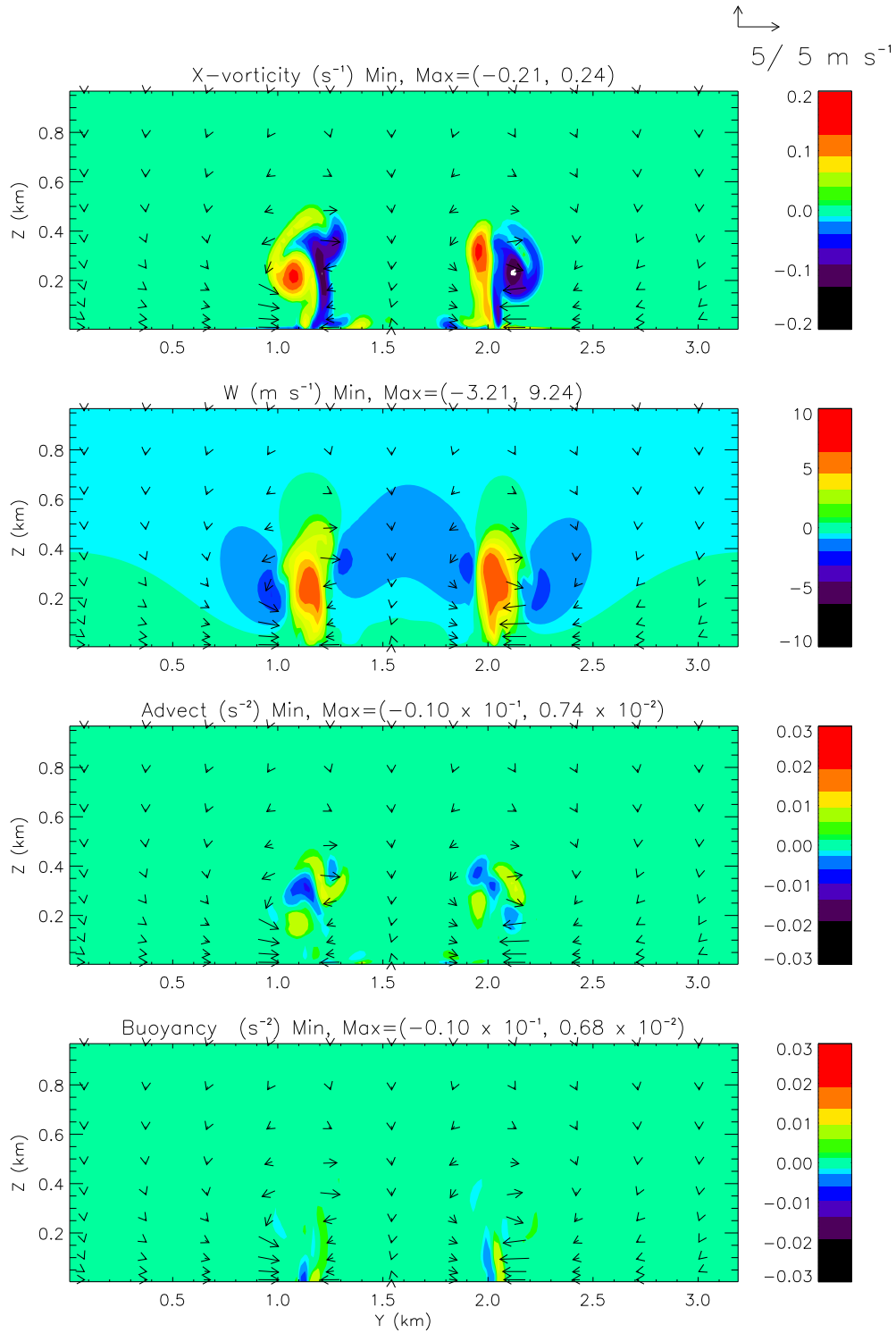


Figure 2: y - z cross sections of terms in linear x vorticity budget Equation (5) for coupled UU-LES experiment GLM-C. The background wind used in this fire simulation is shown (solid line) in Figure 1.

Y Vorticity Budget Time[h:m:s]= 0:14: 0 Section at y(km)= 1.6

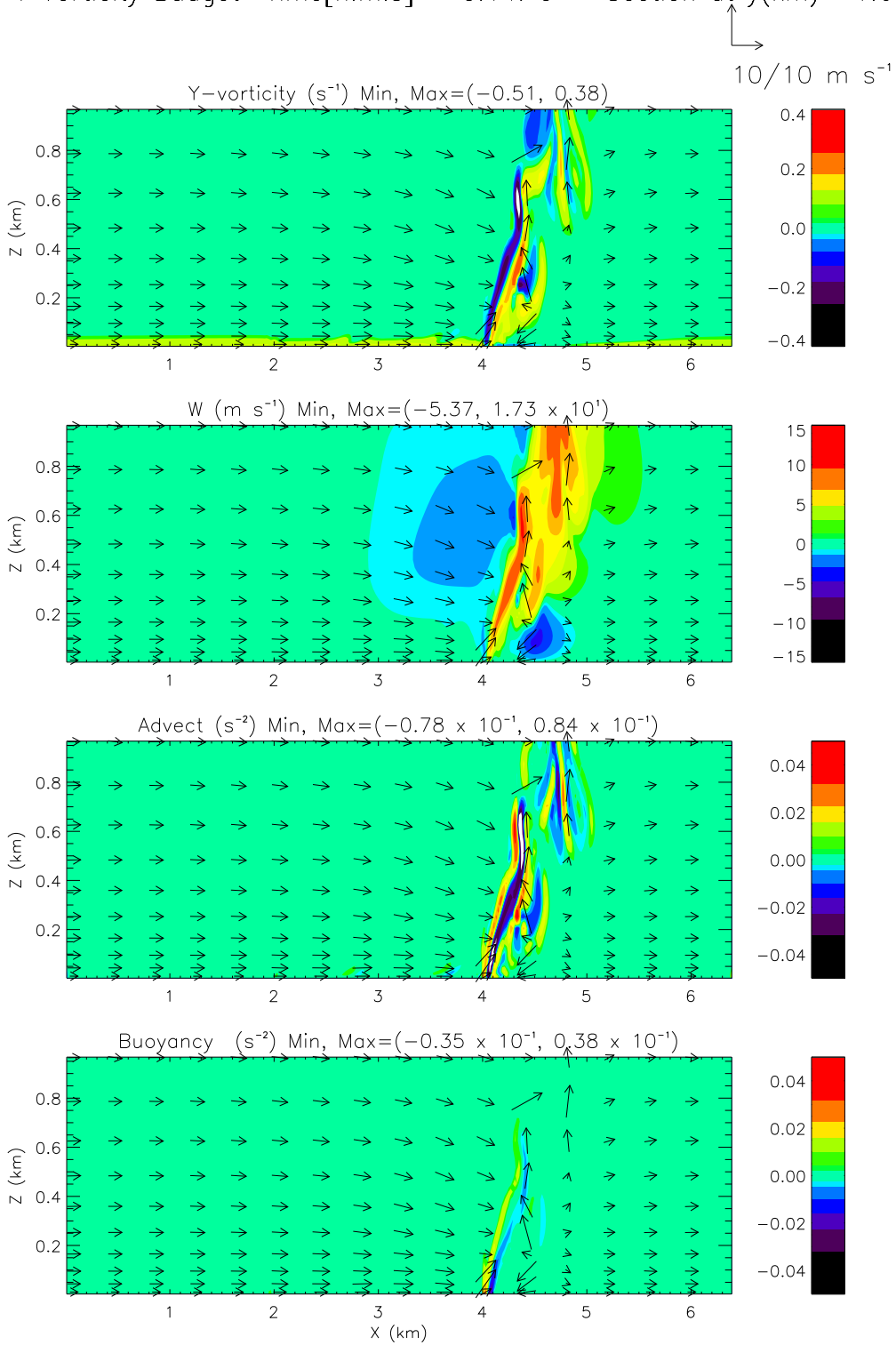


Figure 3: x - z cross sections of terms in linear y vorticity budget Equation (4) for coupled UU-LES experiment GLM-C. The background wind used in this fire simulation is shown (solid line) in Figure 1.

Z Vorticity Budget Time[h:m:s]= 0: 9: 0 Section at z(m)= 53.

↗
5/ 5 m s⁻¹

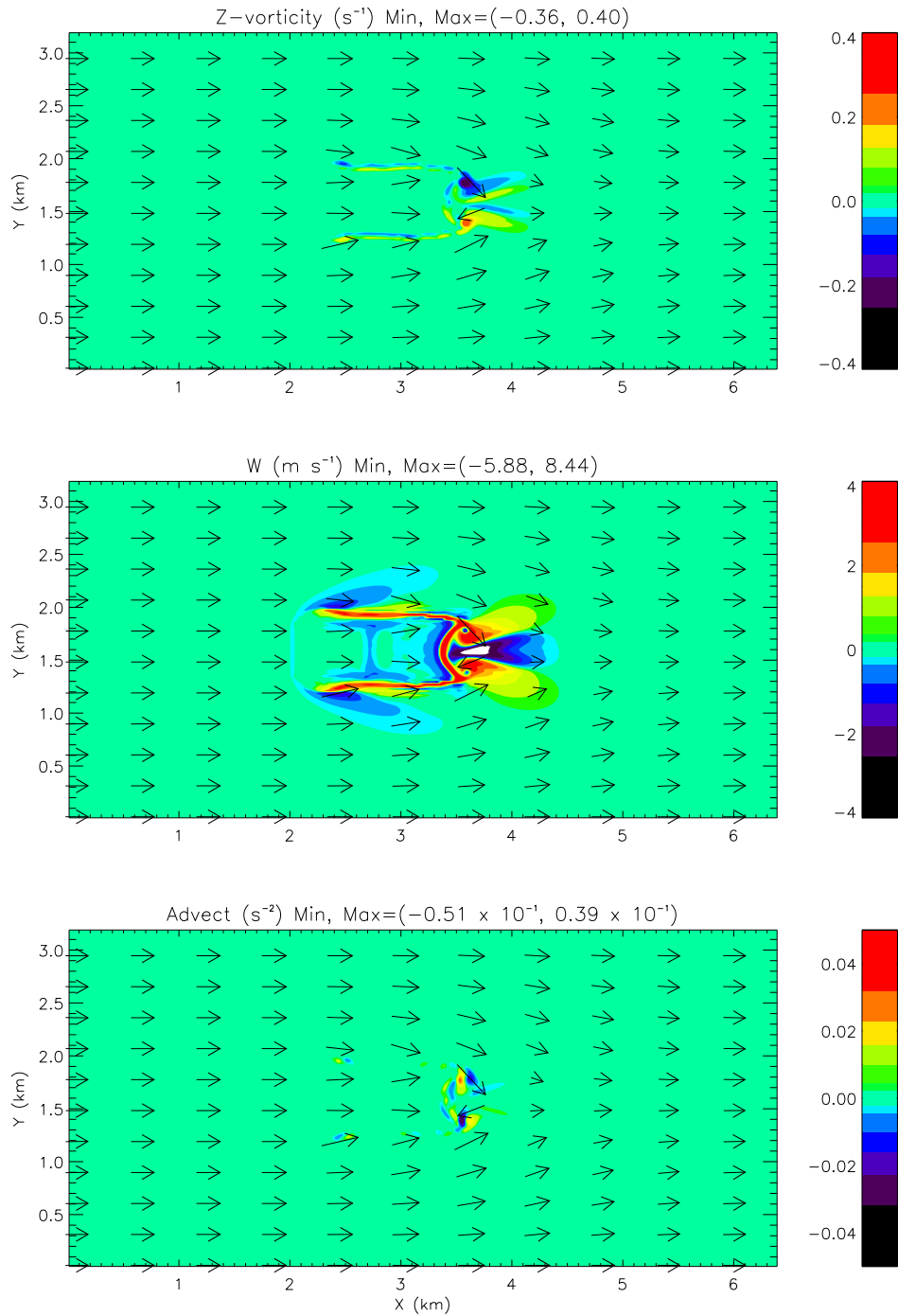


Figure 4: x - y cross sections of terms in linear z vorticity budget Equation (6) for coupled UU-LES experiment GLM-C. The background wind used in this fire simulation is shown (solid line) in Figure 1.

X Vorticity Budget Time[h:m:s]= 0:15: 0 Section at x(km)= 3.2

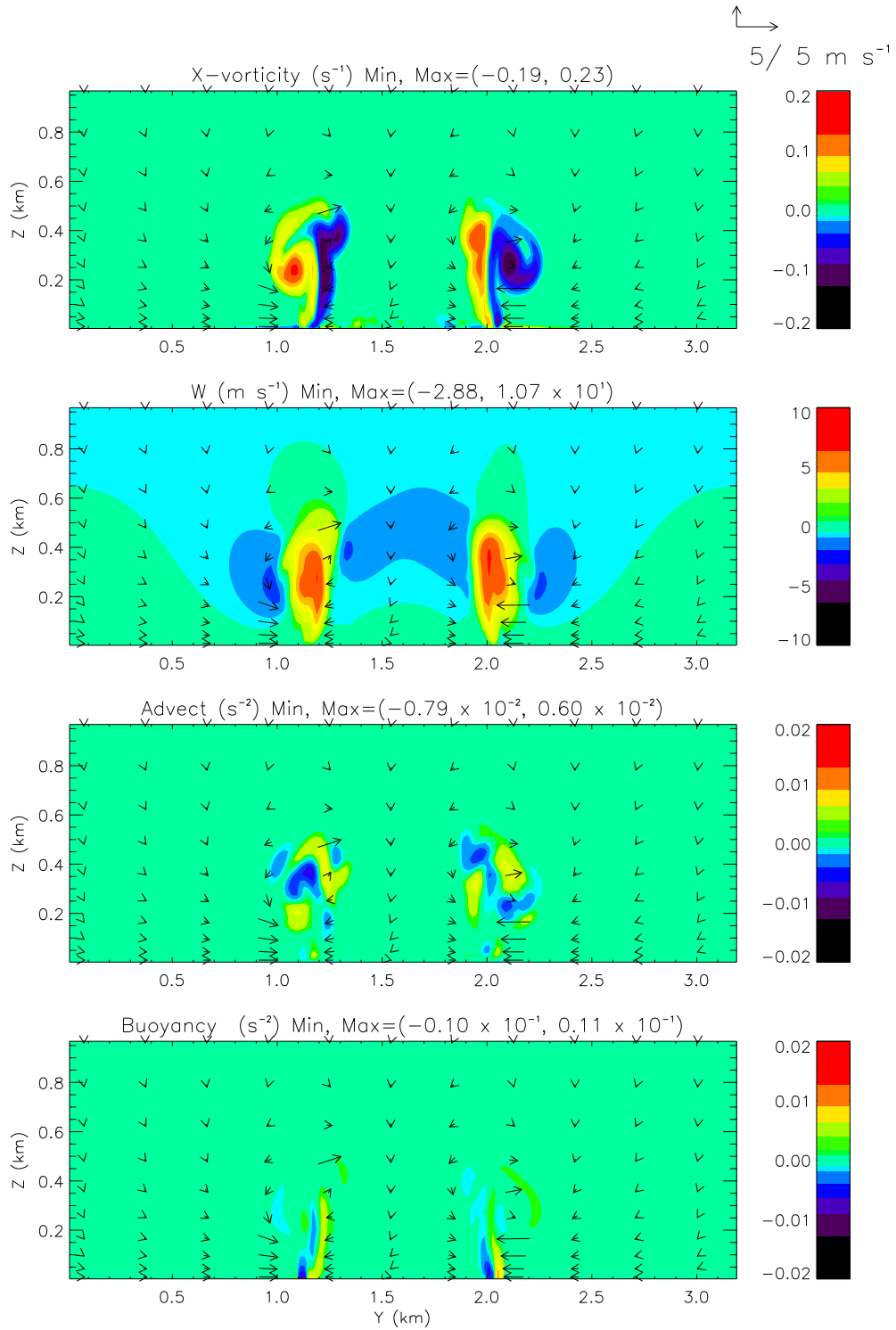


Figure 5: y - z cross sections of terms in linear x vorticity budget Equation (5) for coupled UU-LES experiment GLM-LS. The background wind used in this fire simulation is shown (dotted line) in Figure 1.

Y Vorticity Budget Time[h:m:s]= 0:14: 0 At y(km)= 1.6

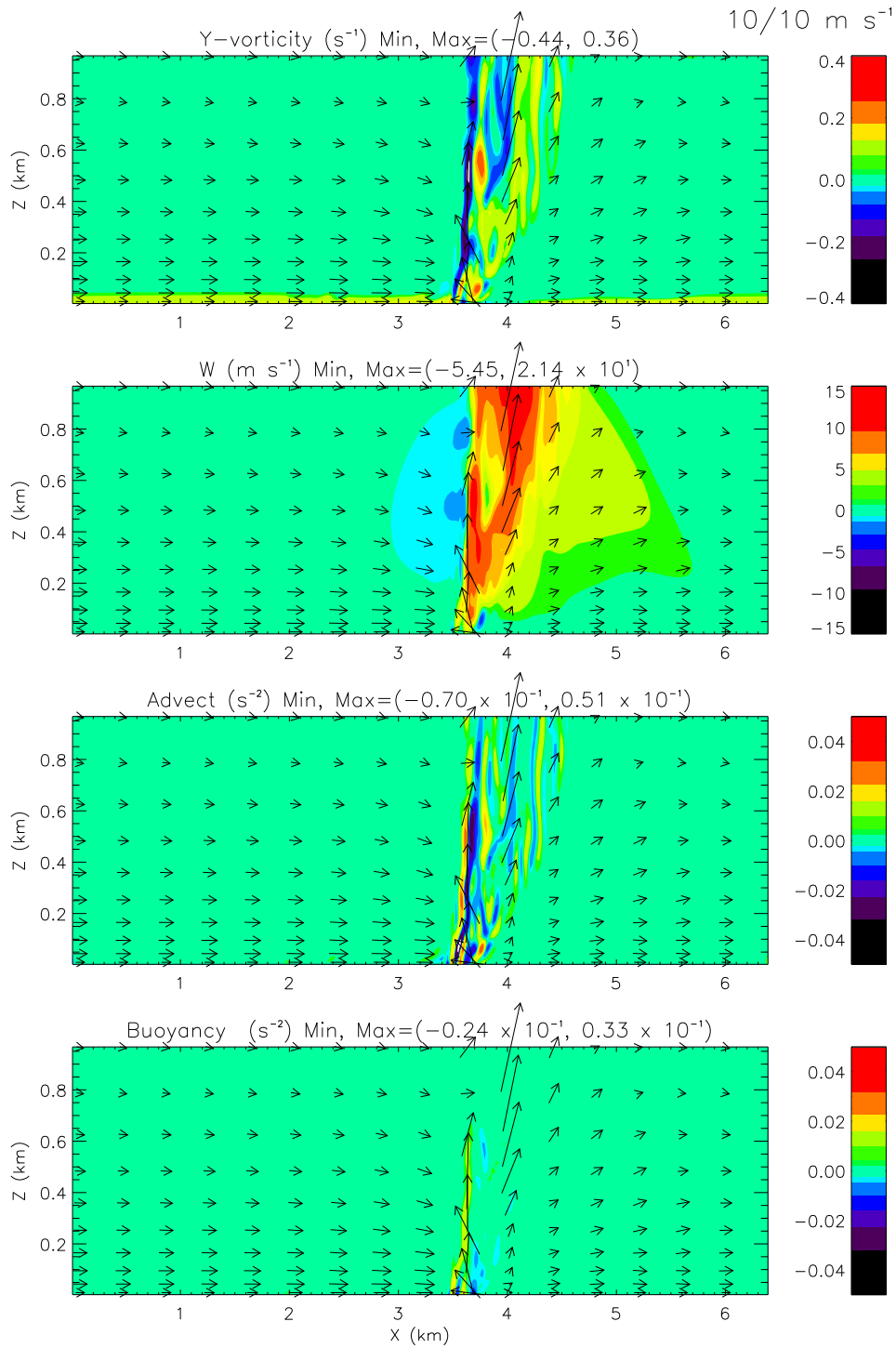


Figure 6: $x-z$ cross sections of terms in linear y vorticity budget Equation (4) for coupled UU-LES experiment GLM-LS. The background wind used in this fire simulation is shown (dotted line) in Figure 1.

Z Vorticity Budget Time[h:m:s]= 0: 9: 0 Section at z(m)= 53.

\nearrow
5/ 5 m s⁻¹

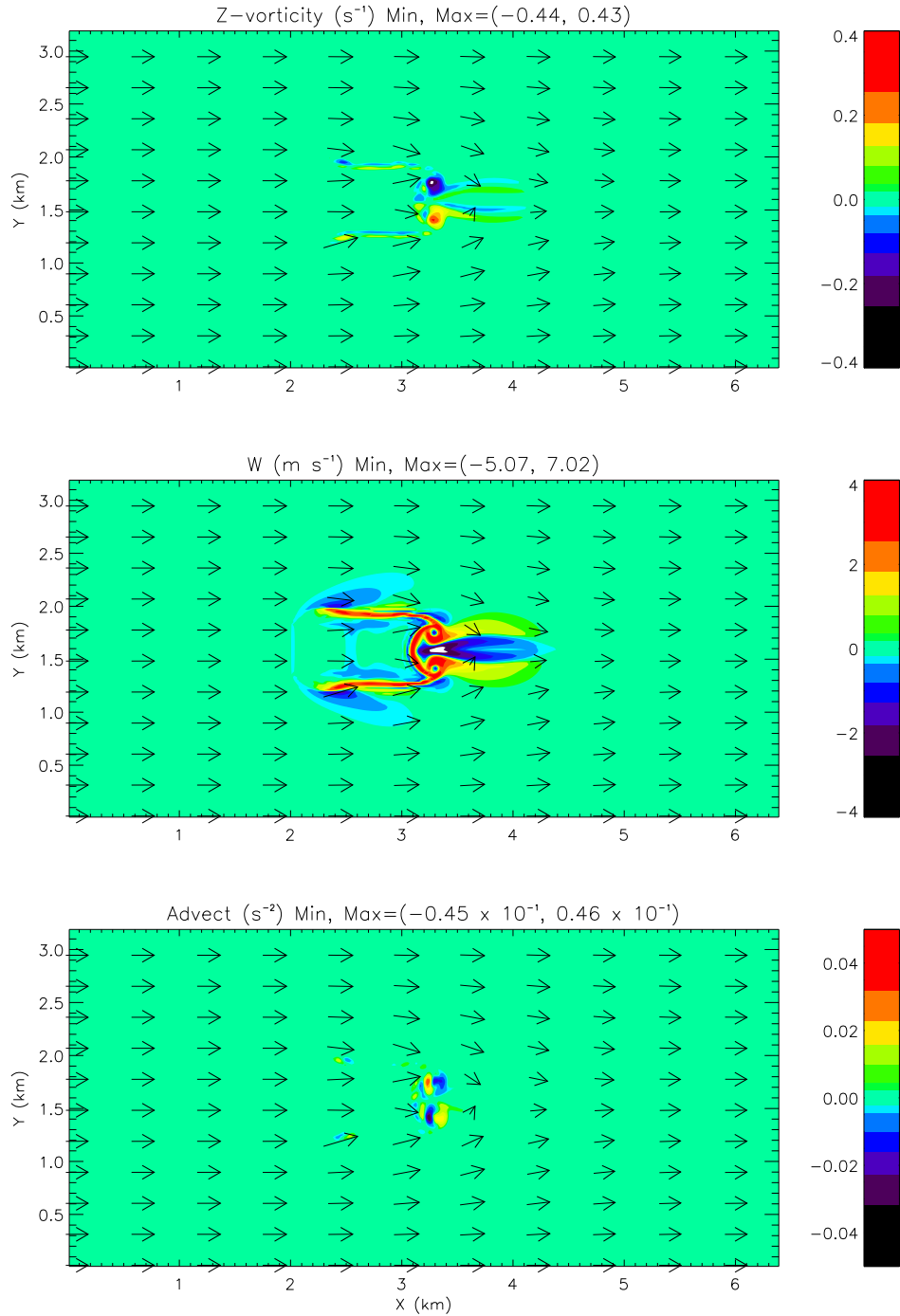


Figure 7: x - y cross sections of terms in linear z vorticity budget Equation (6) for coupled UU-LES experiment GLM-LS. The background wind used in this fire simulation is shown (dotted line) in Figure 1

X Vorticity Budget Time[h:m:s]= 0:15: 0 Section at x(km)= 3.2

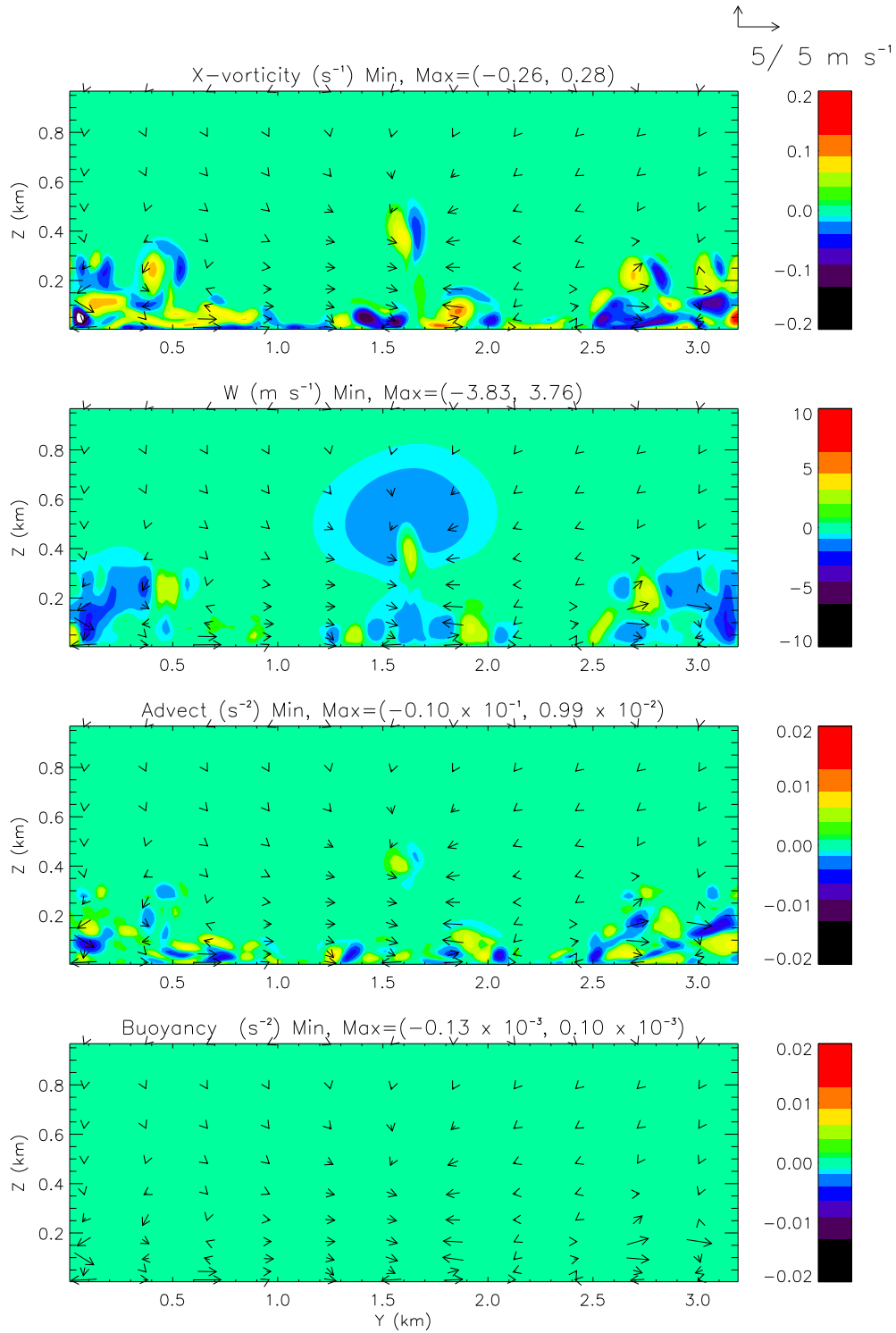


Figure 8: $y-z$ cross sections of terms in linear x vorticity budget Equation (5) for coupled UU-LES experiment GLM-TH. The background wind used in this fire simulation is shown (dashed line) in Figure 1.

Y Vorticity Budget Time[h:m:s]= 0:14: 0 Section at y(km)= 1.6

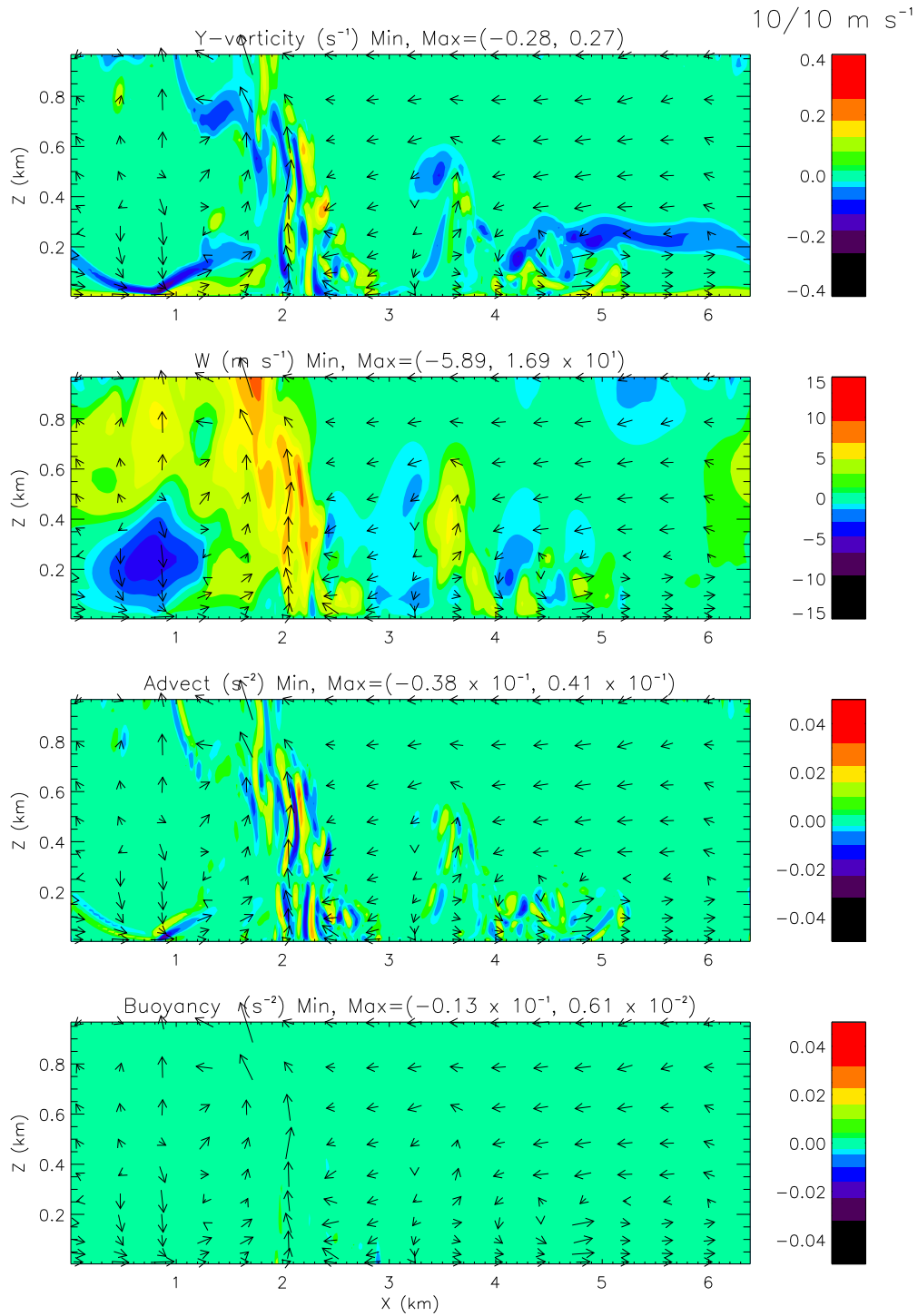


Figure 9: $x-z$ cross sections of terms in linear y vorticity budget Equation (4) for coupled UU-LES experiment GLM-TH. The background wind used in this fire simulation is shown (dashed line) in Figure 1.

Z Vorticity Budget Time[h:m:s]= 0: 9: 0 Section at z(m)= 184.

\nearrow
5/ 5 m s⁻¹

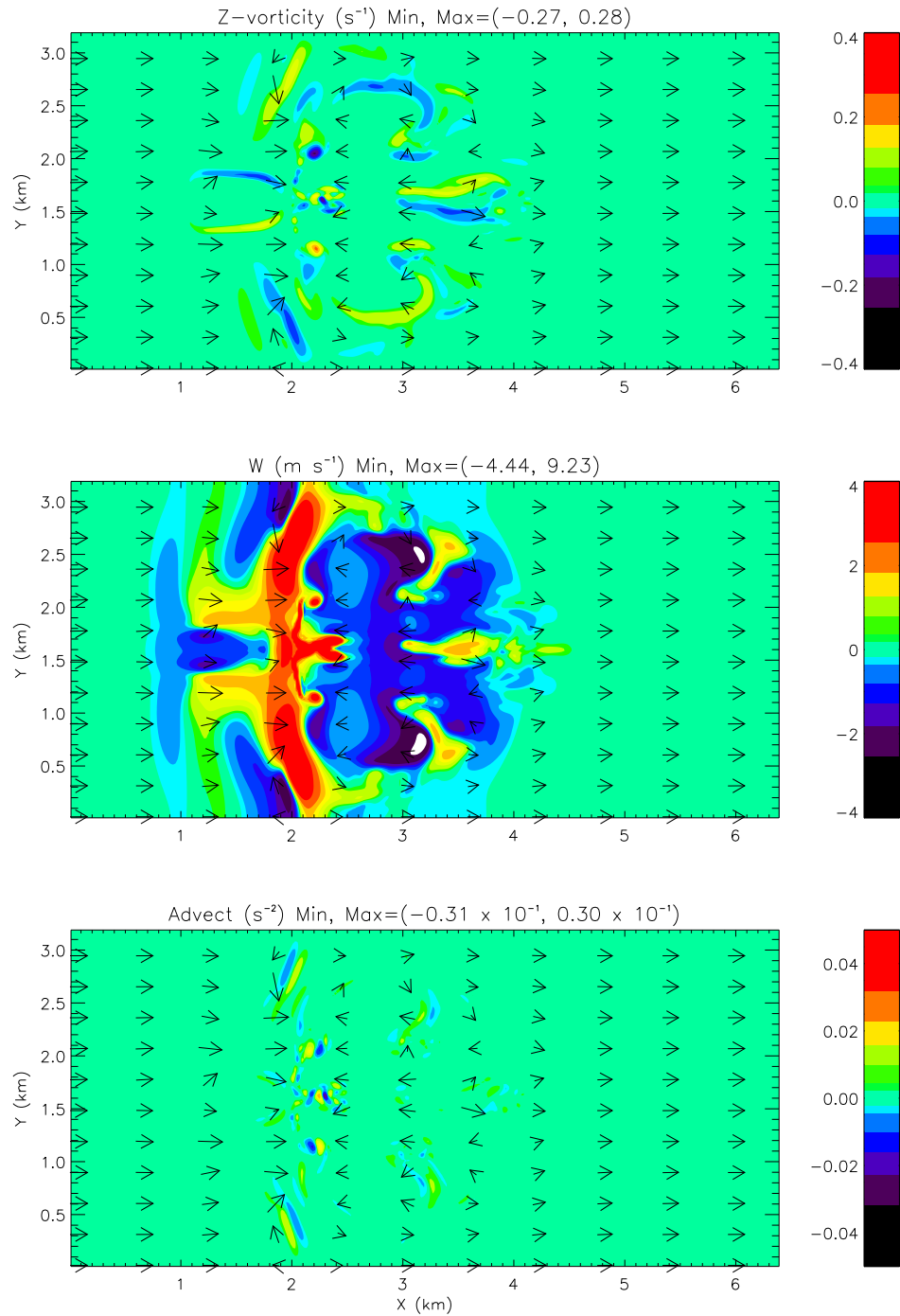


Figure 10: x - y cross sections of terms in linear z vorticity budget Equation (6) for tanh coupled UU-LES experiment GLM-TH. The background wind used in this fire simulation is shown (dashed line) in Figure 1.